Available online at www.sciencedirect.com

SCIENCE DIRECT®

Ecological Modelling 168 (2003) 57–76

ECOLOGICAL MODELLING

www.elsevier.com/locate/ecolmodel

Nonlinear effects of water stress on peanut photosynthesis at crop and leaf scales

R.A. Ferreyra [a,*], J.L. Dardanelli [b], L.B. Pachepsky [c], D.J. Collino [d], P.C. Faustinelli [d], G. Giambastiani [e], V.R. Reddy [f], J.W. Jones [a]

[a] *Agricultural & Biological Engineering Department, P.O. Box 110570, University of Florida, Gainesville, FL 32611-0570, USA*
[b] *E.E.A. Manfredi INTA, RA-5988 Manfredi, Argentina*
[c] *Bldg 007, Rm 125, Hydrology and Remote Sensing Lab, ARS, USDA, 10300 Baltimore Ave, Beltsville, MD 20705, USA*
[d] *INTA IFFIVE, Camino 60 Cuadras Km 5 y 1/2, X 5020 ICA, Córdoba, Argentina*
[e] *Fac. de Ciencias Agropecuarias, Universidad Nacional de Córdoba, Av Valparaiso, S-N, Ciudad Univ, 5000 Córdoba, Argentina*
[f] *Bldg 001, Rm 342A, Alternate Crops & Systems Lab, ARS, USDA, 10300 Baltimore Ave, Beltsville, MD 20705-2350, USA*

Received 29 November 2002; received in revised form 11 April 2003; accepted 12 May 2003

Abstract

Crop models are being increasingly used in agricultural and environmental studies of marginal environments where water availability limits crop growth. The PNUTGRO model (a precursor of CROPGRO and CSM) has systematically underestimated rainfed pod yield and aboveground biomass, while accurately predicting the same variables under irrigation, in the frequently drought-stricken Argentine peanut-growing region. This happened although the model was previously optimized to properly simulate atmospheric water demand and soil/plant water supply, suggesting that the mechanisms of peanut drought tolerance are not adequately expressed in the model.

Crop models such as PNUTGRO typically describe water stress using a linear function to penalize carbon assimilation when water supply falls below a certain limit, assuming that stomatal control affects transpiration and photosynthesis proportionally. We analyzed the feasibility of a linear transpiration—protosynthesis relationship at the leaf and crop scales. At the leaf scale we used two leaf gas exchange models (a conductance model and the anatomy-based 2DLEAF). At the crop scale we replaced the linear equation linking transpiration supply/demand and photosynthesis in PNUTGRO with an equation of the form PG/PGMAX $= 1 - (1 - \text{SWFAC})\text{^WSFEXP}$, where SWFAC is PNUTGRO's transpiration demand/supply ratio and WSFEXP is an empirical nonlinearity constant that was determined by simultaneously fitting simulated and observed biomass and plant-extractable soil water (PESW) content of several field experiments. An independent data set was used for validation.

Both leaf models showed that linearity is infeasible, primarily due to the greater contribution of stomatal aperture to the total pathway resistance of water vapor versus CO_2. At the crop-level, simulations of biomass, PESW, and pod yield in rainfed experiments improved the most when we used the nonlinear function with WSFEXP $= 2.5$. Mean final biomass error improved from -20 to -6.5%; mean final pod yield error went from 20 to 0.07%; mean PESW error went from 5 to -0.2%.

Our results support the idea that water use efficiency (WUE) is a nonlinear function that increases under conditions of water stress. This agrees with experimental evidence from the literature and with theory integrating quasi-steady-state stomatal

* Corresponding author. Tel.: +1-352-392-1864.
E-mail address: aferreyra@agen.ufl.edu (R.A. Ferreyra).

0304-3800/$ – see front matter
doi:10.1016/S0304-3800(03)00195-9

closure due to low soil water availability, short-timescale midday adaptive behavior, and peanut-specific drought-avoidance mechanisms.

Keywords: Crop simulation; Leaf gas exchange; Peanut (*Arachis hypogaea* L.); Water stress; Water use efficiency (WUE); Scaling

1. Introduction

Contemporary crop models such as CSM (Jones et al., 2003), CROPGRO (Boote et al., 1998), GLYCIM (Acock and Trent, 1991), APSIM (Keating et al., 2003), and MACROS (Penning de Vries et al., 1989) are useful tools for studying crop growth and for solving practical agricultural problems such as yield prediction and crop management optimization (Hanks and Ritchie, 1991; Boote et al., 1996; Poluektov and Topaj, 2001). Improved model accuracy and the latest advances in agricultural technologies present new, more sophisticated tasks for crop models, such as understanding genotype by environment interactions and representing variety-specific behavior in the context of new crop varieties that appear in great numbers every year (Smartt and Stalker, 1982; Mavromatis et al., 2001; Hammer et al., 2002).

Extensive practical use of crop models has shown satisfactory results for crops grown under favorable conditions (Boote et al., 1997). However, if the crop encounters stress conditions during its growth period, crop models may perform inadequately (Sau et al., 1999; Calmon et al., 1999). In particular, Ferreyra (1998) found systematic underestimations using PNUTGRO version 1.02 (Boote et al., 1989) to predict rainfed peanut pod yield and aboveground biomass, although the model accurately predicted the same variables under irrigation, and had been optimized to properly simulate atmospheric water demand and soil/plant water supply under rainfed conditions.

Field crops such as rainfed peanut usually experience water stress at least for a short period. For example, Collino et al. (2000) noted that peanut production in Argentina, one of the world's largest peanut exporters, is concentrated in the central semiarid region of Argentina where drought periods are frequent and unpredictable.

The Florman INTA variety was introduced into the region in 1983; its average rainfed yield of over 700 kg was a significant increase compared to previous varieties, so it became one of the predominant cultivars in Argentina (Pedelini, 1991). Simultaneously, an expansion of peanut production area in the region increased peanut yield variability because Florman is quite drought-sensitive (Collino et al., 1994).

Improving the PNUTGRO model's description of the physiological processes involved in drought tolerance is a necessary condition for applying it in yield prediction of drought sensitive varieties such as Florman. The relevant parts of the model where water stress should be coupled must be identified and developed further through a more accurate description of the physiological processes involved. This may be accomplished with downscaling, taking the analysis of growth–water relations to a lower level of crop organization (de Wit, 1982). Thus, if the crop model underestimates canopy-level yield and biomass under stress conditions, we can consider transpiration/photosynthesis relations at the leaf-level. Leaf gas exchange models simulate more physical and biological processes, that is, are more mechanistic than canopy gas exchange models.

There exist a wide variety of leaf-scale models, mechanistic to varying degrees; very few of them have been included into crop models or used for crop model improvement. Marques and Jørgensen (2002) emphasized the need for a more integrative theoretical network in biology and ecology, and Jørgensen's (2002) comment that "ecology does not need to remain a science based on empirical relationships" is applicable to crop science and crop modeling as well. However, a compromise is necessary between the complexity and performance of the crop model enhanced by the incorporation of a lower level of analysis.

In a previous study (Ferreyra et al., 2000), such a compromise between different levels of organization allowed us to approach the calibration of PNUTGRO

1.02 for two very different peanut cultivars having quantitative differences in their leaf anatomy and gas exchange. Leaf-scale analysis showed that an additional, cultivar-specific, leaf anatomy-based parameter was needed to describe varietal differences in transpiration in the crop model.

Peanut leaf gas exchange has been studied several times in the past (Bhagsari and Brown, 1976a,b; Pallas, 1980). Several of these studies included Florunner, a close relative of Florman INTA, under various environmental conditions. Several models of leaf photosynthesis and transpiration also exist (Boote and Loomis, 1991); the model proposed by Farquhar et al. (1980), which describes Rubisco performance and the light reactions of photosynthesis, has repeatedly provided good quantitative descriptions of assimilation and is used in both leaf and canopy levels of organization (Boote and Loomis, 1991). However, when applied to a leaf, the Farquhar model only describes CO_2 assimilation. Transpiration must be estimated using a different method.

Gas diffusion through the boundary layer, stomata and intercellular spaces is usually thought to limit both transpiration and photosynthesis (Parkhurst, 1994). Traditionally, this limitation is presented using an electric analog model based on conductances (Nobel, 1983). The conductance model has been widely used to describe transpiration and, along with Farquhar's model, to describe leaf photosynthesis and its dependence on stomatal control.

In many conductance model implementations the diffusion paths for both CO_2 and water vapor are assumed identical, thus making transpiration and photosynthesis proportional to each other as stomatal aperture changes. This assumption ignores the liquid-phase components of the CO_2 pathway, although Nobel (1983) postulated that liquid-phase conductance values are significant. Parkhurst (1994) criticized conductance models "in part because they are usually one-dimensional representations, but also because they treat continuously interacting processes as if they were sequential." Thus, a lumped-parameter approach, as opposed to using spatially distributed parameters and processes, may introduce error even in the apparently simple simulation of diffusion within intercellular spaces: assimilation really occurs throughout the tortuous intercellular space and concurrently with a gradual fall in CO_2 concentration, rather than lumped at the end of the flow path as in typical conductance models.

However, lumping the properties of the leaf interior was unavoidable until recent developments in numerical methods made it possible to solve diffusion equations in very complex domains. The two-dimensional model of leaf gas exchange 2DLEAF (Pachepsky and Acock, 1996), which explicitly accounts for leaf anatomy, was developed using these methods.

Calculations with 2DLEAF have shown that water vapor and CO_2 concentration distributions in the leaf interior differ from each other (Pachepsky et al., 1995), that photosynthesis and transpiration rates are not proportional to each other, and that stomatal aperture affects transpiration more than it affects photosynthesis (Pachepsky and Acock, 1996), confirming the statement made by Parkhurst (1994), that low stomatal conductance reduces water loss more than it reduces CO_2 uptake.

Several recent studies (Van Wijk et al., 2002; Van den Berg et al., 2002; Tang et al., 2001) have shown that comparing the results of different models and different scales of analysis applied to a particular crop or ecosystem model module can provide valuable insight into the behavior of natural systems. In this study we used two leaf-scale models (a conductance-based model and the leaf anatomy-based 2DLEAF) and a crop-level model (PNUTGRO) with the following objectives:

(1) to investigate whether a linear relationship between the stomatal regulation of photosynthesis and transpiration is feasible (possible) at the leaf scale, and
(2) to use the acquired leaf-scale knowledge, together with field-scale experimental data, to improve the simulation of water stress effects in the PNUTGRO crop model, in order to increase the accuracy of its predictions of biomass and yield in rainfed experiments.

2. Materials and methods

Fig. 1 presents a "roadmap" of the materials used and procedures followed in this study. The paths through the graph are explained in the homonymous sections below.

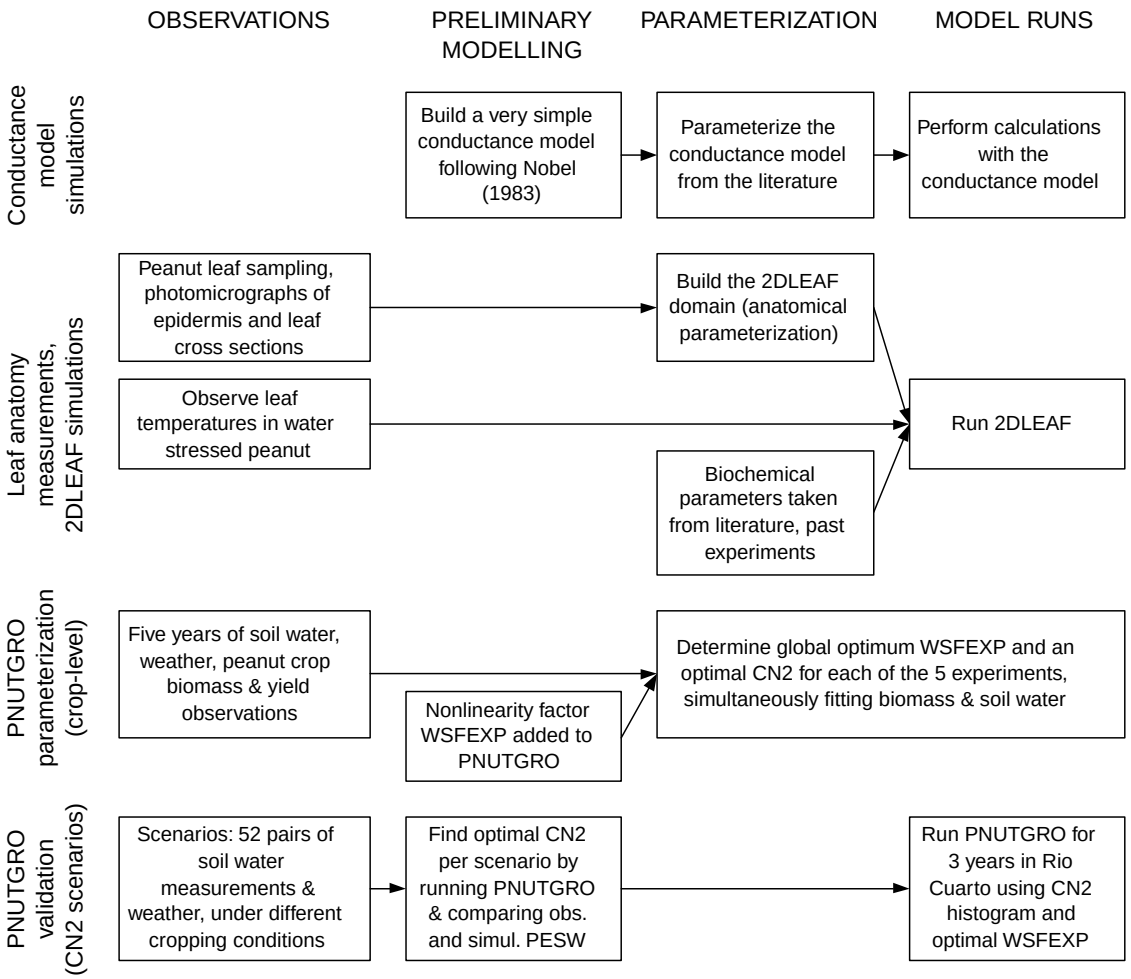

Fig. 1. Data sources and procedures followed in each of the modeling activities.

2.1. Conductance model simulations

The basic assumption of the conductance model is the existence of parameters called conductances (or resistances as reciprocals of conductances) that restrict diffusion of gases within plant tissues or between plant tissues and the turbulent air surrounding the leaf (Fig. 2). Resistances are defined for the intercellular air spaces, the stomata, the cuticle, and the boundary layer adjacent to the leaf. The second assumption is that CO_2 diffuses across the same gaseous-phase resistances as water vapor, and across a number of other liquid-phase resistance components in the mesophyll cells. Using resistances, leaf gas fluxes into and out of leaves can be described by the equations developed for the analysis of electrical circuits.

The third assumption is to describe the gas fluxes across the air boundary layer using a lumped, one-dimensional form of Fick's law of diffusion, replacing the gradual concentration gradient by the difference in concentration across some distance, and introducing a boundary layer conductance, which we will denote $g^{bl}_{H_2O}$. This is a great simplification considering the complex behavior of the boundary layer, a region that is usually described as consisting of two sub-layers. The first layer is the surface region nearest the leaf, "dominated by the shearing stresses originated at some surface in a laminar sub-layer or

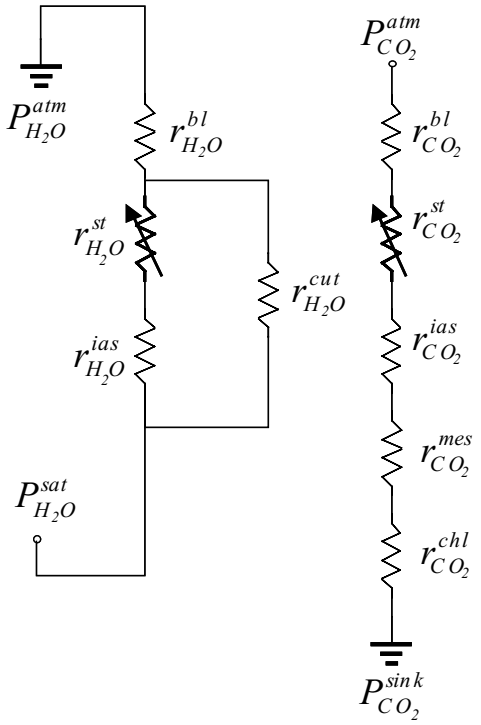

Fig. 2. Electrical analogue of leaf gas exchange pathways. Two gas flux processes are represented: transpiration (left) and CO_2 (right) flux. $P^{atm}_{H_2O}$ and $P^{sat}_{H_2O}$ are the water vapor pressure in atmosphere and on the surface of mesophyll cells, respectively, $P^{atm}_{CO_2}$ and $P^{sink}_{CO_2}$ are CO_2 partial pressure values in the atmosphere and at the carboxylation sites; r^i_j are the resistances to water vapor (j = "H_2O") and carbon dioxide (j = "CO_2") movement in the boundary layer (i = "bl"), in stomata (i = "st"), through the cuticule (i = "cut"), in the intercellular air spaces (i = "ias"), through mesophyll cell walls (i = "mes"), and within chloroplasts (i = "chl").

air where movement is parallel to the leaf surface; air movement is arrested at the surface and has increasing speed at increasing distances" from the leaf surface (Nobel, 1983). The second sub-layer is farther from the surface, and consists of a region of turbulent gas movement.

Nobel (1983) described the diffusion of gases along stomatal pores applying Fick's law and a stomatal conductance (which we will denote $g^{st}_{H_2O}$). This is a widely used parameter in both agricultural and ecological modeling; stomatal conductance refers to the rate of flow per unit area of the leaf, and is considerably easier to measure than the flux density within a stomatal pore. Stomatal conductance is closely related to stomatal aperture. Consequently it is highly variable, especially in natural conditions. In models, time-averaged values are used.

Cuticular conductance, $g^{cut}_{H_2O}$ is probably the most uncertain of all the conductances in this model. Analysis of experimental data showed that cuticular transpiration varies in a wide range for various species. According to a generalization by Larcher (1995), it constitutes 10–33% of the total transpiration, but some researchers presented even higher values. For example, bushes under a forest canopy transpired more than 50% of their total water through the cuticle (Antipov, 1971), and grasses growing in various ecological conditions had cuticular transpiration constituting 16–77% of the total (Antipov, 1978).

The next component of the model is the conductance of intercellular air spaces, $g^{ias}_{H_2O}$. Nobel (1983) proposed calculating this parameter based on the average distance between mesophyll cell surfaces within a leaf and the inner surface of stomatal pores. Consistent application of the conductance model thus would also require measurements on leaf cross-section images.

To simplify the use of the electric analogy, we replaced all conductances with resistances, taking $r^{sp}_{H_2O} = 1/g^{sp}_{H_2O}$, where the superscript "sp" stands for "bl," "st," "cut" or "ias" (boundary layer, stomata, cuticle, and intercellular air space, respectively). The left side of Fig. 2 presents the corresponding equivalent electrical circuit. The cuticular resistance acts as a resistance in parallel with the series sum of the stomatal and intercellular space resistances. According to this scheme, the total leaf resistance to water movement can be described as follows:

$$r^{total}_{H_2O} = \frac{(r^{ias}_{H_2O} + r^{st}_{H_2O})r^{cut}_{H_2O}}{r^{ias}_{H_2O} + r^{st}_{H_2O} + r^{cut}_{H_2O}} + r^{bl}_{H_2O}$$

The electric analogy for photosynthesis can be described in a similar fashion. The path of CO_2 from the surface of mesophyll cells to the carboxylation sites is short but quite complex: the CO_2 molecule must cross the cell wall of the mesophyll cell, the plasmalemma, part of the cytosol, the membranes surrounding the chloroplast, and some of the chloroplast stroma. For each stage of this path a corresponding resistance or conductance can be defined, resulting in numerous parameters having unknown values.

We accounted for this part of the CO_2 pathway using two resistances: mesophyll, $r^{mes}_{CO_2}$, and chloroplast, $r^{chl}_{CO_2}$. The corresponding electrical analogy scheme is presented in the right side of Fig. 2. The corresponding equation for the total resistance, $r^{total}_{CO_2}$, can be expressed as

$$r^{total}_{CO_2} = r^{bl}_{CO_2} + r^{st}_{CO_2} + r^{ias}_{CO_2} + r^{mes}_{CO_2} + r^{chl}_{CO_2}$$

where the superscripts "bl," "st," and "ias" correspond to the boundary layer, stomatal, and intercellular spaces components, respectively.

All resistances were calculated from the typical conductance values provided by Nobel (1983) as follows (all in mmol m^{-2} s^{-1}): $g^{bl}_{H_2O} = 1500$; $g^{st}_{H_2O} = 0.2, \ldots, 200$; $g^{ias}_{H_2O} = 2000$; $g^{cut}_{H_2O} = 10$; $g^{bl}_{CO_2} = 937.5$; $g^{st}_{CO_2} = 0.125, \ldots, 125$; $g^{ias}_{CO_2} = 1250$; $g^{mes}_{CO_2} = 66$; and $g^{chl}_{CO_2} = 100$. Values of water vapor flux $Flux_{H_2O} \propto g^{total}_{H_2O}$, and the CO_2 flux $Flux_{CO_2} \propto g^{total}_{CO_2}$ were calculated for the range of stomatal conductance values assuming that the other conductances remain constant.

2.2. Leaf anatomy measurements

Leaf samples were collected from an experiment conducted in 1999/2000 at the INTA Institute of Phytopathology and Plant Physiology (IFFIVE), Córdoba, Argentina (31° 24′ S, 61° 11′ W, elevation 474 m). The Florman INTA variety was grown under well-watered conditions: the fraction of available root zone water content was kept above 60%.

Ten leaflets were sampled from the crop on the 55th day after planting for the analysis of adaxial and abaxial leaf surfaces as well as leaf cross-sections. The leaflets were collected from the first fully expanded and fully developed leaf (usually the second or third from the apex) on the main stem of randomly selected plants. Epidermal samples were obtained by mechanical peeling from the abaxial and adaxial surfaces of the leaflets. Leaf cross-section samples were obtained with a microtome following treatment with xylol and inclusion in paraffin. Two kinds of coloration were performed: (a) double, using saffranin/fast-green (Ma et al., 1992) and (b) toluidine blue (Sakai, 1973). The prepared slides were observed with a magnification of 200× under a Zeiss Axiophot microscope with imaging capabilities, which was also used to digitize the resulting images. Leaf cross-section and epidermal images (Fig. 3) were scanned using Optimas 6.1 software and the software package SigmaScan was used to measure the cell sizes of different tissues, as well as the thickness and volume of the leaves and their tissues. The results of these measurements were summarized in the leaf cross-section schematization (Fig. 4) that was used as the domain for calculations with the 2DLEAF model.

2.3. 2DLEAF simulations

The two-dimensional model of leaf gas exchange 2DLEAF was described in detail by Pachepsky and Acock (1996) and has been employed in ecological (Pachepsky and Acock, 1996), physiological (Pachepsky et al., 1997), biophysical (Pachepsky et al., 1999) and crop simulation (Ferreyra et al., 2000) studies. The model simulates (a) transport of CO_2, O_2 and water vapor in the intercellular spaces and in the boundary layer adjacent to a leaf, (b) fluxes of CO_2, O_2 and water vapor across the cell surfaces driven by the difference between atmospheric and intercellular concentrations. Assimilation of CO_2 and evaporation of water are simulated on the surfaces of the polygons representing palisade and spongy mesophyll cells. Values of CO_2 concentration at the outer edge of the boundary layer are equated to the ambient CO_2 value. Water vapor pressure at the cell surfaces is set to the standard saturation value for the given leaf temperature. The domain for solving the diffusion equation is different for water vapor and CO_2 because of peanut's very particular leaf anatomy: it has large water storage cells adjacent to the abaxial surface (Fig. 3). Water evaporation occurs from their surfaces, but not CO_2 assimilation. Assimilation of carbon dioxide is described in 2DLEAF using the model described by Farquhar et al. (1980), accounting for temperature, CO_2 concentration and light intensity.

The main assumptions of the 2DLEAF model are:

(a) Three-dimensional gas flow is approximated in two dimensions.
(b) In leaf cross-section schematizations, the real shapes of palisade and spongy cells are replaced with rectangular approximations. Palisade cell widths vary in our simulation domain, with their distribution close to the observed one, but the

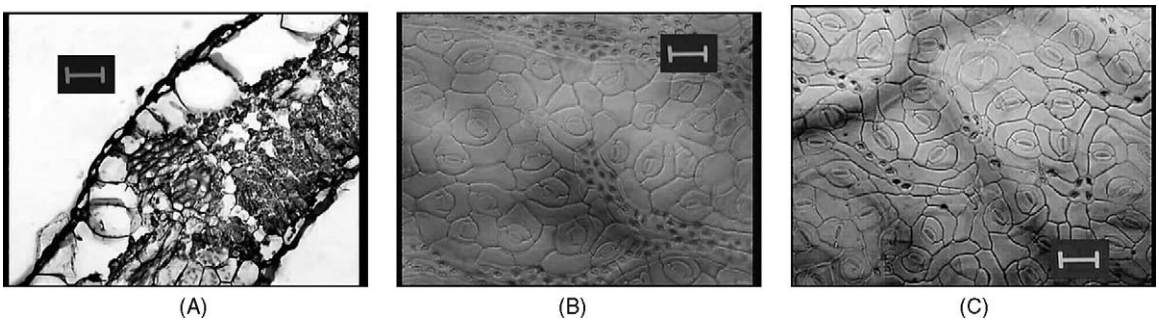

Fig. 3. Example of leaf cross-section (A) and epidermal photomicrographs of the adaxial (B) and abaxial (C) leaf surfaces. The marks are 58 μm long.

lengths of the palisade cells were assumed constant, and equal to the measured palisade tissue thickness; the size of spongy cells also varied.

(c) All the mesophyll cell surfaces in the domain absorb CO_2 for assimilation.

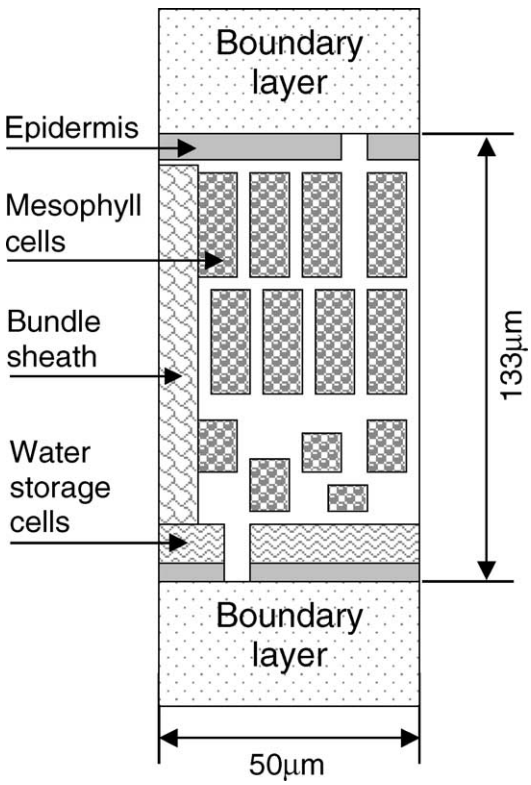

Fig. 4. Schematization used for the 2DLEAF simulations, obtained from the observed data.

(d) Boundary layers can be described by two parameters: a thickness d, and an effective diffusion coefficient D_{ef}, equal for both sides of the leaf.

(e) Stomata are distributed uniformly on the leaf surface, but with different density on the abaxial and adaxial surfaces.

(f) CO_2 assimilation occurs on the cell surfaces, and CO_2 transfer inside cells was not considered.

The system of equations of the model includes three diffusion equations with different boundary conditions for all three gases. It is solved numerically using a Galerkin-type finite element method, as detailed by Pachepsky and Acock (1996).

We parameterized 2DLEAF for peanut quantifying using measurements from numerous leaf cross-sections and epidermal peels. Fig. 4 presents the resulting simulation domain. Biochemical parameters were determined for peanut in our previous study (Ferreyra et al., 2000). Parameters of the gas transport sub-model and of the carbon assimilation sub-model depend on temperature; the gas diffusion coefficient, D_g, values depend on temperature, T (K), as follows:

$$D_g = D_{0,st}\left(\frac{T}{273.15}\right)^a$$

where $D_{0,st}$ is the molecular diffusion coefficient at 760 mmHg atmospheric pressure and 273.15 K, and a is a parameter ranging from 1.75 to 2 (American Institute of Physics Handbook, 1972). Dependencies of biochemical parameters on temperature are assumed to obey Arrhenius-type equations as suggested by Harley and Tenhunen (1991).

We ran 2DLEAF for different combinations of leaf temperature and stomatal apertures assuming an incident radiation of 2000 $\mu mol\,m^{-2}\,s^{-1}$. In order to obtain realistic leaf temperature values for our simulations, we measured leaf temperature of water stressed (using mobile rainout shelters), and well-irrigated Florman plants during the 1997–1998 cropping season in IFFIVE. Leaf temperature was measured at noon using a Horiba IT 330 infrared thermometer (Horiba, Japan) sensitive to the thermal radiation in the 6–12 μm wavelength band. The measured temperature values were regularly checked using a portable blackbody standard accurate to the nearest 0.1 °C. We used representative values to determine the range of temperatures used in the 2DLEAF simulations, and in graphs where stomatal aperture and temperature were not considered independent variables, we assumed that temperature varied between the two temperature extremes as a linear function (with a negative slope) of transpiration, that is, maximum latent heat loss corresponded to minimum temperature, and vice versa.

2.4. Crop-level experiments

Experiments were conducted at the INTA Manfredi Experimental Station, Manfredi, Argentina (31° 49′ S, 63° 48′ W, elevation 292 m); and at the National University of Córdoba, Faculty of Agronomy, Córdoba, Argentina (31° 30′ S, 64° 00′ W, elevation 360 m). We also used data reported by Seiler and Vinocur (1995) near the Río Cuarto region (33° 12′ S, 64° 23′ W, elevation 421 m). The soil in Manfredi and Córdoba is a silty loam Enthic Haplustoll, whereas in Río Cuarto it is an Entic Hapludoll (USDA Soil Taxonomy). All of these soils have A, AC, and C horizons, a silt content ranging from 60 to 70%, and a pH of 7.1–7.7. The soil profiles do not present any physical constraints to root development. Planting dates, row spacing and plant populations are presented in Table 1. Weeds were eliminated by hand. Foliar diseases and spider mites were controlled by regular application of fungicides and insecticides recommended by the INTA Extension Service, Argentina. A completely randomized design with three to four replicates was used for each experiment.

The (drained) upper and lower soil water holding limits per soil layer at each site (DUL and LL, respectively) were obtained using the procedure suggested by Ritchie (1981). The lower limits were usually reached only at shallower soil layers (0–100 cm), but were extrapolated to greater depths because the soil properties throughout the C horizon were relatively constant. The volumetric water content at saturation was determined in the laboratory. Soil water content was measured in each plot every 2–10 days. The gravimetric technique was used in the upper 10 cm, and a neutron probe was used at 20 cm intervals between the depths of 10 and 230 cm. Daily weather measurements (maximum and minimum air temperature, relative sunshine fraction for solar radiation estimations), were recorded approximately 100–1000 m away from each experimental site. Daily rainfall was measured with a rain gauge closer to the experimental plots. All above ground biomass, including pods when present, was harvested 5–7 times during the crop-growing cycle from 1.5 m^2 sub-plots, oven-dried and weighed.

2.5. The PNUTGRO model

PNUTGRO was described in detail by Boote et al. (1989). The model simulates, with a daily time step, the biomass accumulation, leaf area, phenology, and soil water balance of a peanut crop, assuming no nutrient limitations. It uses daily weather data.

For this study we used the model with the management parameters shown in Table 1, and Florman INTA genetic coefficients obtained by Ravelo and Dardanelli (1992) and Seiler and Vinocur (1995). We previously optimized PNUTGRO using (a) irrigated experiments to accurately predict crop potential evapotranspiration, and (b) experiments with an imposed drought period to obtain rooting depth and root distribution parameters to maximize the accuracy of soil evaporation and plant transpiration simulations under supply-limited conditions. Ferreyra (1998) provided a detailed description of this process.

Fig. 5 shows a simplified diagram of the interactions between water balance and biomass production implemented in PNUTGRO 1.02. Of particular interest is the role of the two parameters, the U.S. Soil Conservation Service (SCS) runoff curve number CN (SCS, 1972), and the proposed nonlinearity factor WSFEXP. Both parameters are described in detail below.

Table 1
Description of the PNUTGRO parameter estimation experiments

Site	Experiment	Planting date	Plant population (m^{-2})[a]	No. data points[b]	Weight[c]	CN2 (linear)[d]	CN2 (nonlinear)[e]
Manfredi	RAMA9001	5 December 1990	15.8	12/17	1/1	93	93
Manfredi	RAMA9101	27 November 1991	15.8	10/30	1/1	90	91
Manfredi	RAMA9302	17 November 1993	12.2	7/18	1/1	92	93
Manfredi	RAMA9404	22 November 1994	11.9	5/15	1/1	90	91
FA	RAUN9301	20 November 1993	11.9	4/6	1/1	93	94

[a] Row spacing was 70 cm for all the experiments.
[b] Number of data points available in each experiment for biomass/PESW.
[c] Weight applied to the experiment's biomass/PESW in the objective function.
[d] Optimal value of the CN2 curve number for each experiment in the linear (WSFEXP = 1) case.
[e] Optimal value of the CN2 curve number for each experiment in the nonlinear (WSFEXP = 2.5) case.

The SCS curve number is a parameter that lumps the effects of multiple phenomena that control runoff (rainfall intensity and soil cover, for example) into one value that describes the behavior of the system throughout a period of interest. The equation linking rainfall, CN and runoff for a rainfall event is the following:

$$R = \frac{[P - 0.2((25400/\mathrm{CN}) - 254)]^2}{P + 0.8((25400/\mathrm{CN}) - 254)}$$
$$\text{if } P > 0.2\left(\frac{25400}{\mathrm{CN}} - 254\right), \quad R = 0 \text{ otherwise}, \quad (1)$$

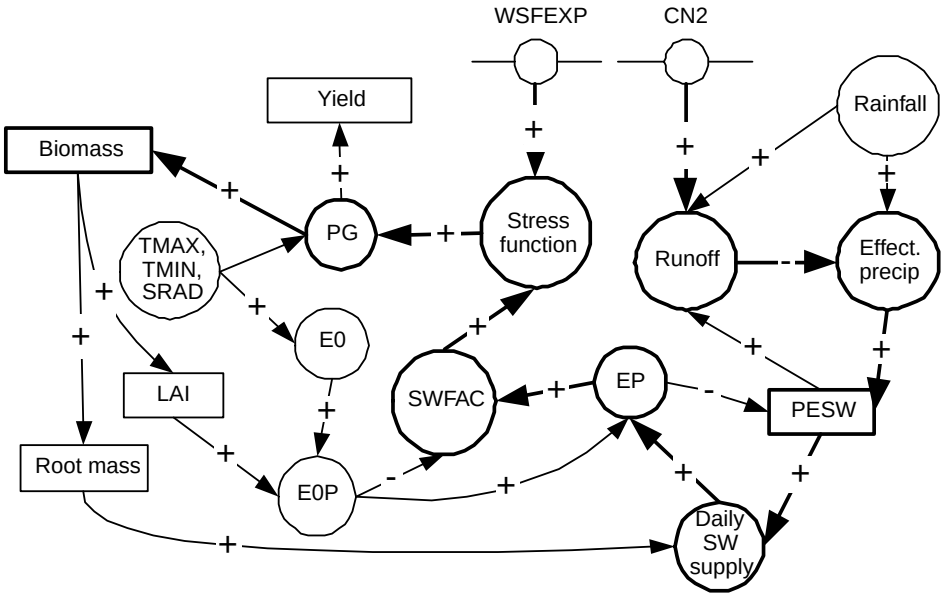

Fig. 5. Simplified causal diagram of the interaction between the water balance and photosynthesis modules of the modified PNUTGRO model. Abbreviations: SW, soil water; PESW, plant extractable soil water; E0, potential evapotranspiration; EOP, potential transpiration; EP, actual transpiration; SWFAC, PNUTGRO's existing soil water supply/demand ratio; PG, gross photosynthesis; LAI, leaf area index; TMAX, maximum daily temperature; TMIN, minimum daily temperature; SRAD, solar radiation; CN2, mean SCS runoff curve number; and WSFEXP, proposed nonlinearity factor. The paths leading from the parameters used in the simultaneous optimization and the observed soil water and biomass are marked with darker lines. Note the negative feedback from biomass to PESW through the LAI → EOP → EP and through root mass → daily SW supply → EP. The presence of feedback requires the simultaneous estimation of the two parameters, CN2 and WSFEXP.

where R is runoff and P is precipitation, both in mm, and CN takes values from 0 to 100.

Although the SCS Hydrology Handbook (SCS, 1972) provides tables for estimating CN2 (a "mean" value of CN over the period of interest) according to land cover, slope, tillage, etc., the effective value of CN2 for any particular cropping season is a priori unknown because it depends on the intensity of all the individual rainfall events. The effect of this uncertainty on simulated water balance is especially strong at the higher range of CN2 values, such as in the Haplustolls of central Argentina, which tend to crust (Hall et al., 1992).

The function linking water stress to photosynthesis in the original PNUTGRO (and in its successor, CROPGRO) is linear and consists of the factor SWFAC, the ratio between water supply (by the soil through the root system) and water demand (by transpiration), limited to a maximum value of 1. This factor is calculated on a daily basis and multiplied by a calculated potential daily gross photosynthesis.

We instead proposed an empirical nonlinear water stress function, shown in Eq. (2), which takes SWFAC as input. Its derivative with respect to SWFAC is shown in Eq. (3):

$$\text{Water stress function} = 1 - (1 - \text{SWFAC})^{\text{WSFEXP}} \tag{2}$$

$$\frac{\partial \text{Water stress function}}{\partial \text{SWFAC}} = \text{WSFEXP}(1 - \text{SWFAC})^{\text{WSFEXP}-1} \tag{3}$$

The shape of this function for different values of the WSFEXP parameter is shown in Fig. 6. We chose this function because it complies with two important conditions:

(a) When WSFEXP = 1, the function collapses back into the original linear function.
(b) Except for the special case in which WSFEXP = 1, the derivative of the water stress function with respect to SWFAC is always 0 when SWFAC = 1. This represents the assumption that the water stress avoidance mechanisms of crop plants should result in an insignificant variation of photosynthesis for small levels of nonsatisfaction of optimum daily water requirements.

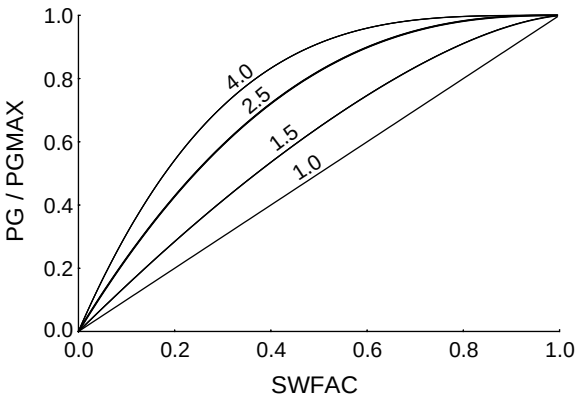

Fig. 6. Proposed function linking gross photosynthesis and satisfaction of transpiration requirements, PG/PGMAX = 1 − (1 − EP/EPMAX)^WSFEXP, for different values of the WSFEXP parameter.

Assuming that evapotranspiration ET is estimated accurately, and that there is no drainage from the bottom of the profile, then a value of CN2 may be estimated using a two-step procedure: first, given a difference in total soil water content ΔPESW from successive measurements of soil water content in the profile, estimate runoff using R = P − ET − ΔPESW, and then search for the value of CN2 that best fits the runoff estimate and measured rainfall in Eq. (1). Similarly, given a series of measurements of soil water content in the profile, and assuming that LAI and potential net photosynthesis can be simulated accurately, then Eq. (2) can be parameterized by searching for the value of WSFEXP that best fits the series of observed values of total biomass.

The scheme described above has problems. Measuring total biomass (including total root mass) is impractical; only aboveground biomass is determined in typical modeling experiments. Root mass must therefore be estimated. Moreover, the allocation of photosynthates to the root system is water stress dependent in peanut (Wright et al., 1994), and changes in root length density will affect the crop's ability to extract water from the profile and thus will feed back to plant-extractable soil water (PESW). Furthermore, changing WSFEXP will impact biomass and leaf area, so water demand may also change. Thus, there is feedback from biomass to PESW (Fig. 5), so CN2 and WSFEXP cannot be estimated independently. This motivated the simultaneous approach described below.

2.6. PNUTGRO parameter estimation

We set up the process to obtain a single optimal WSFEXP value across all the experiments, considering it a characteristic of the Florman genotype. An optimal CN2 was calculated for each experiment, accounting for the variability of CN2 over space and time. The objective function of the estimation process was defined as the weighted sum of ten (2 per experiment) squared terms. Five of the squared terms corresponded to relative biomass errors (difference between predicted and observed biomass, divided by the observed value) and the other five to relative PESW errors (difference between predicted and observed PESW, divided by the mean value of PESW for the whole experiment). Using relative errors allowed us to combine different variables and different years in one same objective function. Equal weights were applied to the relative errors of biomass and PESW of the five calibration experiments. This was done despite the different number of measurements per variable and experiment. The discussion elaborates on the implications of different weighting schemes. The total number of measurements per variable per experiment is shown in Table 1. A flowchart of the parameter estimation process is shown in Fig. 7.

2.7. PNUTGRO validation

In order to provide independent validation for the predictive capability of the modified model given the fact that WSFEXP and CN2 were fitted simultaneously, we performed additional crop-scale validation as follows:

(1) We estimated typical CN2 runoff curve number values in the region by fitting observed & simulated water balance over a large number of short-term, mostly fallow scenarios observed over several years in Manfredi and not used in the calibration process. Fig. 8 shows the distribution of CN2 values over these scenarios.
(2) In order to test the value of WSFEXP without simultaneously fitting CN2, the PNUTGRO model was used to run multiple simulations in Río Cuarto for each of the RARC9201, RARC9301, and RARC9401 experiments shown in Table 2, assigning CN2 to each run according to the histogram of CN2 values obtained above for the Manfredi scenarios, an environment with a rainfall regime to similar to that of Rio Cuarto. We did this while keeping WSFEXP constant at its optimal level. The distributions of simulated pod yield and biomass were compared with the values reported by Seiler and Vinocur (1995).

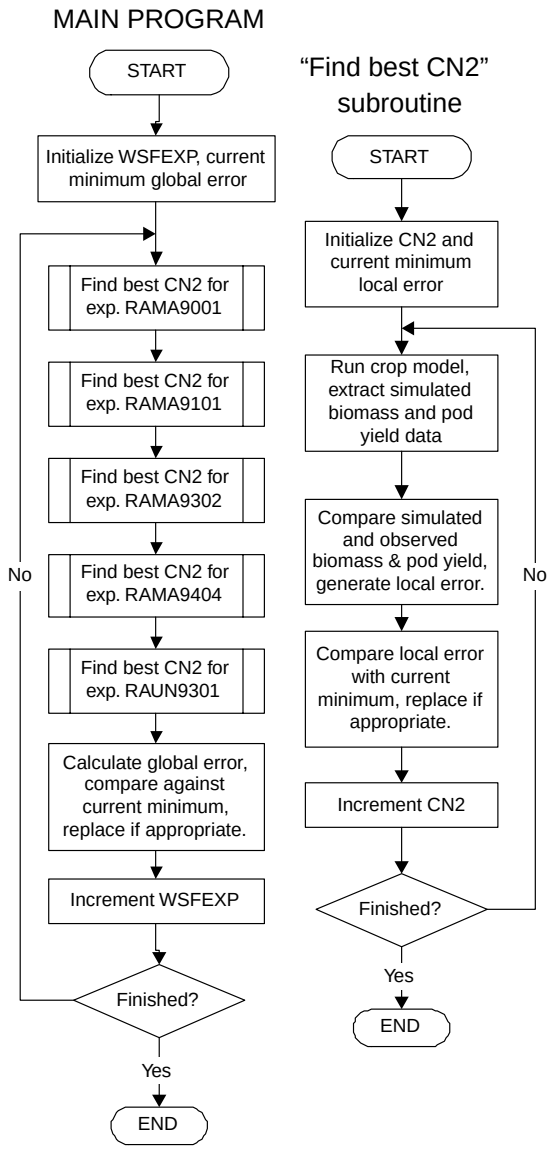

Fig. 7. Flowchart of the PNUTGRO parameter estimation process.

Table 2
Description of the PNUTGRO validation experiments

Site	Experiment	Planting date	Plant population (m^{-2})[a]	Simulated biomass[b] (kg ha^{-1})	Observed biomass (kg ha^{-1})	Simulated pod yield[b] (kg ha^{-1})	Observed pod yield (kg ha^{-1})
Rio IV	RARC9201	5 December 1992	12.0	3775 ± 2022	5381	1807 ± 981	2590
Rio IV	RARC9301	8 December 1993	12.0	8492 ± 2207	6608	4497 ± 1234	3586
Rio IV	RARC9401	3 December 1994	15.5	5755 ± 1627	7330	2056 ± 978	2358

[a] Row spacing was 70 cm for all the experiments.
[b] Shown in the form mean ± standard deviation.

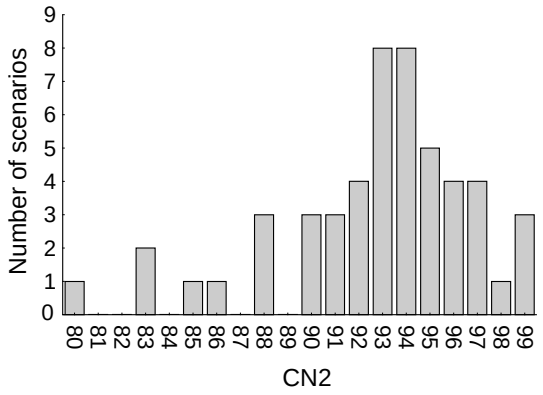

Fig. 8. Histogram of CN2 values obtained in the validation scenarios.

3. Results

3.1. Anatomical data and leaf-scale modeling

Table 3 presents the image analysis results of leaf cross-sections and abaxial and adaxial surfaces of peanut (cv. Florman INTA) leaves. Leaf thickness varied between 130 and 140 μm with a mean of 133 μm. Water storage, bundle sheath, and mesophyll cell areas were present in a proportion of 12, 15 and 51%, respectively, with the remaining 11% occupied by epidermal tissue. The number of palisade cells was slightly higher than the number of spongy cells, and the palisade cells were approximately 3 times larger than the spongy cells. Cell area index (Pachepsky and Acock, 1996), an important descriptor of the photosynthetic capacity of the leaf, was not very high: 16.5. Stomatal density was slightly higher on the adaxial leaf surface versus the abaxial surface. Stomata were quite long, about 20 μm, with the ability to open up to 12 μm wide.

Fig. 9 presents example 2DLEAF results, the dependence of simulated water vapor and CO_2 fluxes on stomatal aperture for three different temperatures, 20, 30 and 42 °C. The fluxes are normalized with respect to their maximum values. As stomatal aperture decreases, both fluxes decrease, but the response of transpiration is significantly stronger than that of photosynthesis at the three tested temperatures. Fig. 10 presents conductance model results, the dependency of water vapor and CO_2 fluxes on stomatal conductance. Both variables are normalized with respect to their maximum values, that is, the values corresponding to fully open stomata. Transpiration rate and photosynthesis showed, respectively, linear and nonlinear relationships with stomatal conductance.

Table 3
Measured and calculated characteristics of peanut (*Arachis hypogaea* L.) cv. Florman INTA leaves, per 200 μm of leaf cross-section sample length

No.	Characteristic	Mean ± S.E.
1	Leaf thickness (μm)	133 ± 5.1
2	Percentage area of water storage cells	12.3 ± 1.7
3	Percentage area of bundle sheath	15.2 ± 2.3
4	Number of palisade mesophyll cells	27 ± 1.3
5	Mean area of palisade call (μm^2)	245 ± 13.7
6	Mean perimeter of palisade cell (μm)	82 ± 4.1
7	Number of spongy palisade cells	21 ± 1.1
8	Mean area of spongy cell (μm^2)	79 ± 7.6
9	Mean perimeter of spongy cell (μm)	35 ± 3.1
10	Cell area index, CAI	16.5
11	Stomatal density, SD, abaxial (mm^{-2})	247 ± 48
12	Stomatal density, SD, adaxial (mm^{-2})	273 ± 42.3
13	Length of stomate, abaxial and adaxial (μm)	19.5 ± 1.8
14	Width of stomate, abaxial and adaxial (μm)	11.8 ± 1.5

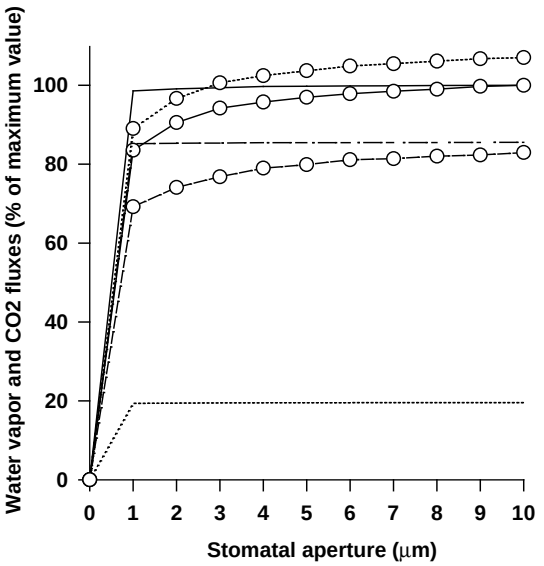

Fig. 9. Dependencies of water vapor flux (lines with circles) and CO_2 assimilation (solid lines) steady state fluxes on stomatal aperture at 35 °C (lines), 20 °C (dashed lines), and 42 °C (dotted lines), calculated with 2DLEAF on the domain constructed from observed leaf anatomy data. The *y*-axis ratio is expressed with respect to maximum stomatal aperture at 35 °C.

3.2. Crop-scale modeling and PNUTGRO parameter estimation

The mean values of final biomass and pod yield of the PNUTGRO simulations of the calibration experiments (Table 1) using the default linear case

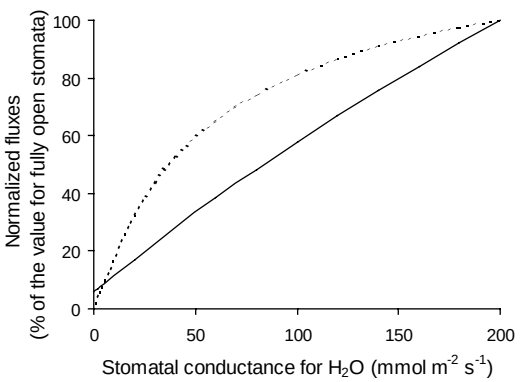

Fig. 10. Dependencies of water vapor (solid line) and CO_2 (dotted line) fluxes on stomatal conductance, as obtained using the conductance model shown in Fig. 2.

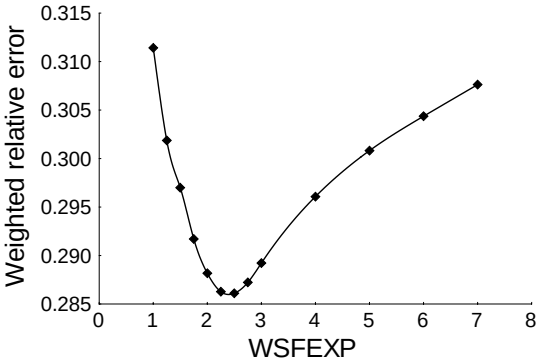

Fig. 11. Objective function used in the optimization process. The weighted relative error and WSFEXP are adimensional variables.

(WSFEXP = 1) were 6597 kg ha^{-1} (biomass) and 3124 kg ha^{-1} (pod yield), whereas the observed mean final biomass and pod yield were 7753 and 3772 kg ha^{-1}, respectively, a first indicator of biomass underestimation in the original model.

Fig. 11 shows the value of the objective function versus the corresponding value of WSFEXP. The value that minimized error, that is, the optimum, corresponded to WSFEXP = 2.5, which we will call the nonlinear case. The corresponding optimal values of CN2 for the five experiments are shown in Table 1. The biomass and PESW residuals (predicted − observed values) for all the individual measurements of the five experiments in the linear and nonlinear cases are shown in Figs. 12 and 13 opposite the corresponding observed values. The model underestimated biomass ($\bar{y} = -360.1$ kg ha^{-1}, S.E. = 49.1 kg ha^{-1}, $n = 35$), and overestimated PESW ($\bar{y} = 5.55$ mm, S.E. = 2.13 mm, $n = 86$) in the linear case; the simulation visibly improved in the nonlinear case for both biomass ($\bar{y} = -246.5$ kg ha^{-1}, S.E. = 119.85 kg ha^{-1}, $n = 35$) and PESW ($\bar{y} = -2.16$ mm, S.E. = 2.14 mm, $n = 86$). The nonlinear case's mean simulated final biomass was 7260 kg ha^{-1}. Thus, final biomass underestimation was reduced from 18 to 6.5%, and average PESW changed from a 5% overestimation to a negligible underestimation.

The residuals in both cases of Figs. 12 and 13 seemed to have a trend. In the case of biomass residuals, linear case, $y = 442.8 - 0.1799x$, $R^2 = 0.32$, *P*-value = 0.0004. For the nonlinear case, $y = 103.5 - 0.0784x$, $R^2 = 0.094$, *P*-value = 0.074. For

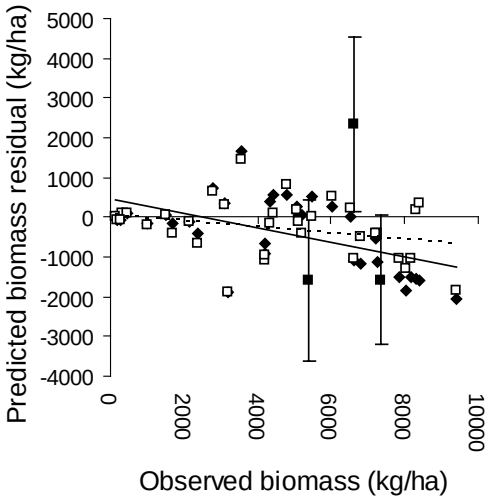

Fig. 12. Scatterplot of biomass residuals for the linear case (WSFEXP = 1, solid diamonds, solid trend line) and nonlinear case (WSFEXP = 2.5, hollow squares, dotted trend line) of five experiments. The bars show the mean and standard deviations of 52 simulations run with different CN2 values for each of three validation experiments in Río Cuarto.

PESW residuals, linear case, $y = -1.96 + 0.0631x$, $R^2 = 0.041$, P-value $= 0.061$; for the nonlinear PESW case, $y = -10.43 + 0.0695x$, $R^2 = 0.049$, P-value $= 0.040$.

Fig. 14 shows the relationship between CO_2 and H_2O flux ratios for the two leaf-level models and for

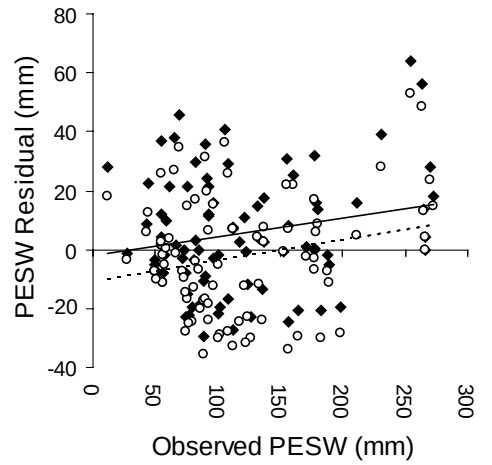

Fig. 13. PESW residual scatterplot for WSFEXP = 1.0 (solid diamonds, solid trend line) and WSFEXP = 2.5 (hollow circles, dotted trend line) over the five calibration experiments.

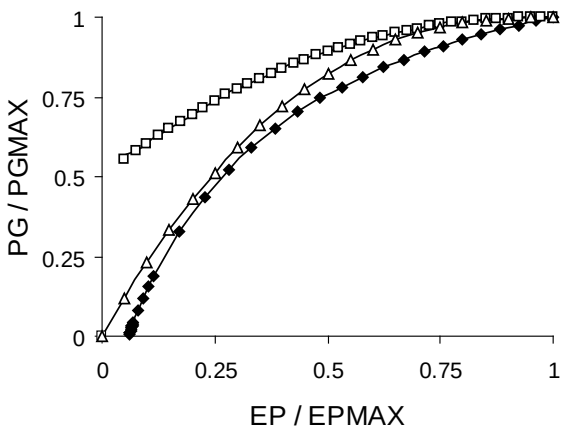

Fig. 14. Relative gross photosynthesis vs. relative transpiration calculated with the conductance model (black diamonds), 2DLEAF (white squares), and the PNUTGRO nonlinear case (white triangles).

the nonlinear (WSFEXP = 2.5) case of PNUTGRO. In each case the x-axis shows the ratio of actual transpiration to a nominal (in our case, maximum) value, and the y-axis presents the corresponding CO_2 flux ratios.

Finally, a note regarding pod yield, which in peanut crop simulation is usually of greater interest than biomass and PESW. The pod yield variable did not participate in any way in the parameter estimation process. However, the accuracy of its simulation changed even more significantly than that of biomass and PESW. In the linear case, mean simulated final pod yield was 3124 kg ha^{-1} over all the experiments, versus 3772 kg ha^{-1} mean observed final pod yield, an underestimation of 20%, slightly greater than that of biomass. In the nonlinear case, mean simulated final pod yield was 3775 kg ha^{-1}, practically identical to the observed value.

3.3. Validation scenarios

Fig. 12 shows the observed values of biomass of the three validation experiments together with bars indicating the standard deviation of the 52 simulations run for each experiment using the 52 CN2 values shown in Fig. 8. These values, together with the three experiments' observed pod yields and simulated pod yield means and standard deviations, are shown in Table 2.

4. Discussion

4.1. Anatomical data and leaf-scale modeling

The results of the anatomical measurements shown in Table 3 do not differ significantly from those of an earlier set also made with Florman INTA (Ferreyra et al., 2000). All characteristics remained within 5% across the different dates, although the two experiments were grown in different years and under different conditions. This stability of Florman anatomical features is encouraging, lending further support to the idea proposed by Ferreyra et al. (2000), that leaf-level modeling can be used to assist crop model parameterization; these authors observed significant anatomical differences between leaves of cultivars with different drought tolerance levels, and correspondence between those differences and simulated gas exchange behaviors at the leaf-level.

The 2DLEAF results shown in Fig. 9 and the conductance model results shown in Fig. 10 are consistent with the idea presented by Parkhurst (1994) that stomatal aperture affects transpiration more than it affects photosynthesis.

Fig. 14 shows the fluxes calculated with the conductance model and 2DLEAF expressed relative to the maximum fluxes, together with the crop-scale PG/PGMAX relationship implemented in PNUTGRO with the optimal WSFEXP = 2.5. The temperature extremes taken for the 2DLEAF simulations were 30 and 42 °C. Note how the conductance, 2DLEAF, and optimized PNUTGRO curves are all nonlinear, consistent with the idea that gross photosynthesis is affected less by nonsatisfaction of transpiration requirements than would be expected under the linear relationship between SWFAC and PG originally implemented in PNUTGRO.

The conductance model shown in Fig. 2 is far simpler than the 2DLEAF simulation, since it does not consider different temperature scenarios, an actual photosynthesis model, etc. but it does clearly show that a linear relationship between photosynthesis and transpiration is infeasible. It can be assumed that in the boundary layer and across the stomata resistances to the flow of water vapor and CO_2 are proportional, linked by the ratio of molecular weights of the two gases, but similarity stops there. The intercellular air spaces that must be traversed by water vapor and by CO_2 are different: water can flow from nearby cells to replenish the water necessary to maintain saturated conditions in the substomatal cavity, but CO_2 must diffuse towards assimilation sites into the most distant recesses of the mesophyll. Thus, the mean distance that a CO_2 molecule must travel (and hence its equivalent resistance in the conductance model) is proportionally greater for CO_2 than for water vapor. Furthermore, as reported by Nobel (1983), the liquid-phase components of the CO_2 pathway components have significant nonzero values, so even if cuticular resistance were infinite, it is impossible for the stomatal component of the gas transport pathways to be the same fraction of the total, and thus, linearity is infeasible.

4.2. Crop-level experiment optimization and validation

Basing the objective function shown in Fig. 11 on relative errors made it possible for us to combine errors across different variables and experiments. Moreover, it addressed the issue that minimizing root-mean-squared error (RMSE) to fit a regression curve through biomass data within an experiment is misleading because the variance of the data is a function of their magnitude, that is, the age of the crop. An immediate precursor of our approach is the peanut model parameterization process implemented by Young et al. (1979), where three variables (top mass, pod weight, and flower count) were combined into one objective function using the same scheme, albeit for one year at a time rather than the five years used in this study. Similarly to Young's objective function, ours arbitrarily assigns equal weights to each experiment–variable combination; we weighted equally the relative errors in biomass and soil water content of all the experiments, regardless of the number of data points contained in each.

The selection of a weighing scheme can affect the results; for example, if the errors of the experiment–variable combinations (RAMA9001 biomass, RAMA9101 PESW, etc.) had been weighted proportionally to the number of data points contributed by each combination as shown in Table 1, the optimal WSFEXP would have been 3.0, but if the first three experiments had all been given a weight of 1, and the last two experiments, which have less data, had been

weighted with 0.75 and 0.5, the optimal WSFEXP would be 2.25. We avoided considering the amount of data per experiment because favoring one year more than others may bias the parameter estimation process towards a solution that simulates crop yield better under weather conditions corresponding to the year(s) with more data. It is thus desirable to have a good mix of wet and dry years in the parameter estimation processes.

Fig. 12 shows how, even in the nonlinear case, the model continues to underestimate biomass, albeit to a far lesser extent than in the linear case. This is related primarily to the simultaneous fitting of biomass and PESW. Equal weight was given to goodness-of-fit of both variables with the intent of avoiding an artificially good fit of biomass while disregarding the fit of PESW, the limiting factor for biomass production in the region. Switching to WSFEXP = 2.5 did produce a simultaneous improvement in the goodness-of-fit of both variables, but further room for improvement is possible, as is suggested by the slight underestimation of both PESW and biomass after the optimization process. We believe that explicitly incorporating a physically-based simulation of the effect of soil water content dependent mechanical impedance on pegging and pod formation would improve results further. Since the peanut seed has a high lipid and protein content, its carbon costs are high compared to those of leaves and stems (Penning de Vries et al., 1974), thus a change in pod yield due to mechanical impedance would have a magnified opposite effect on biomass due to the differences in carbon costs between seeds and vegetative tissue. This effect is currently not modeled in PNUTGRO or its successors CROPGRO and CSM, and could be particularly noteworthy in very dry experiments, in which the soil of the pegging region (topsoil layer where peanut reproductive organs form) would be hardest. The five experiments used in the calibration stage represent different levels of water stress, biomass, etc. and indeed RAMA9001, the driest of the experiments, had the greatest discrepancies between the optimal fit for PESW and the optimal fit for biomass.

The optimal values of CN2 obtained for the five experiments shown in Table 1 seem very high compared to the values tabulated by the SCS (1972), but they are nonetheless consistent with Central Argentina's high summer rainfall intensity and crusting-prone soils (Hall et al., 1992; Ferreyra, 1998). However, the common technique implemented in PNUTGRO and many other crop models of assigning a unique value of CN2 to a location based on land cover, etc. runs into an important limitation: the curve number is also dependent on rainfall intensity (Boughton, 1989), which may vary seasonally and interannually in the region of interest. Note the trend in the residuals in both of the cases shown in Fig. 13. This trend is probably not an artifact of the optimization method, but rather a manifestation of the problems associated with having a constant curve number. The five calibration experiments had a time course of PESW typical of the region: PESW is maximum in November/December, and decreases throughout the summer as precipitation is exceeded by evapotranspiration. Rainfall intensity behavior is also seasonally variable. The precipitation regime in the early season (late spring) is strongly convective, thus rainfall intensity and CN2 are high. Contrarily, low-intensity precipitation from stratiform clouds predominates during the late season (early autumn). Since PNUTGRO and similar models only use a unique value of CN2 for the entire season, in Central Argentina the models will tend to overestimate PESW in the early season when PESW is high (right side of Fig. 13), and underestimate it in the late season when it is low (left side of Fig. 13).

It is interesting to note in Table 1 that in the benchmark (linear) case of WSFEXP = 1, the optimization algorithm yields values of CN2 that are generally lower than the ones corresponding to WSFEXP = 2.5. The differences shown are small, but in the high range of curve number values, there can be large changes in simulated runoff corresponding to CN2 values one unit apart: in the case of the five calibration experiments, the difference ranged between 7.9 and 15.6% increase in total runoff over the whole cropping season.

The above shows how, in the absence of a proper simulation of the nonlinear effect of water stress on biomass production, the CN2 optimization process attempts to explain the higher-than-expected biomass by infiltrating extra water. Indeed, as shown in Eq. (1) and in Fig. 5, a lower CN2 implies lower runoff, thus greater infiltration/effective rainfall, thus greater soil water content, less water stress, and more biomass. Using WSFEXP = 1, we assign the wrong cause to a given observed effect, that is, arbitrarily simulating an increased water supply instead of a greater water

use efficiency (WUE; Tanner and Sinclair, 1983), and hence the positive bias in the WSFEXP = 1 case in Fig. 13. This problem can plague crop models when using an inverse modeling approach to search for the optimal parameter combination to explain observed results. The predictive capabilities of the calibrated model may subsequently be poor even if the calibration process fit the observed data extremely well.

The three validation-specific bars included in Fig. 12 show the impact of naturally occurring variability of high-range CN2 values (and the predictive uncertainty associated with it) on biomass. This influence increases with lower biomass due to the effect of greater water limitation, in which case biomass becomes more dependent on CN2-associated variations of infiltration. Indeed, the coefficients of variation (CVs) of biomass are 54, 27, and 25% for the three validation bars going from left to right, and the CVs for pod yield (bars not shown) are 54, 48 and 27%. Note also how the standard deviation bars touch the zero-error line, suggesting that the validation results are consistent with the observed distribution of CN2 values in the region.

4.3. Water use efficiency

Based on the nonlinear relationships shown in Fig. 14, we postulate that under conditions of water stress, the dry matter/transpired water ratio or crop transpiration WUE of peanut rises. This is consistent with the findings of Craufurd et al. (1999), who measured transpiration efficiency in potted peanut plants while preventing water loss through soil evaporation, and concluded that water deficit (50% versus 100% maximum available soil water) increased WUE at two different fixed temperatures (27 and 34 °C).

The idea of greater water stress accompanied by greater WUE also agrees with the findings of Abbate et al. (2002), who, analyzing the relationship between biomass and water consumption during periods of high light interception (during which transpiration is the dominant water-loss phenomenon), found that the relative decrease in biomass due to water stress with respect to a relative decrease in water consumption is nonlinear, having a similar shape to that found in this study. Their results arose from experiments conducted in multiple sites throughout the world under very different environmental conditions.

Sinclair et al. (1984) stated that stomatal control acting to prevent high transpiration rates could significantly improve WUE. In particular, they postulated that stomatal closure during midday periods of high evaporative demand would be a very useful strategy for increasing WUE. The nonlinearity we have observed at the crop scale integrates numerous causes: on one hand, it has been shown how leaf anatomy supports the idea of a variable WUE; on the other, Eq. (2) using WSFEXP = 2.5 must also integrate observed phenomena such as the quasi-steady-state stomatal closure due to low soil water availability; the short-timescale midday adaptive behavior suggested by Sinclair et al. (1984); and peanut-specific drought-avoidance mechanisms such as heliotropism that reduces light interception, increases leaf reflectivity due to the exposure of the lighter abaxial surface, reduces leaf temperature, decreases the vapor pressure gradient on the adaxial surface that becomes folded over itself, etc.

Based on the different mechanisms incorporated into each of the models, we do not attempt to compare quantitatively the three curves shown in Fig. 14. However, we find it valuable to compare our crop-level curve with an equivalent curve that could be drawn from the results of Abbate et al. (2002). The existence of peanut-specific drought-avoidance mechanisms may help to explain the differences in curvature between Abbate's relationship for wheat, which shows a 39% increase of relative gross photosynthesis with respect to the 1:1 line at the equivalent of SWFAC = 0.5, and ours for peanut, which for WSFEXP = 2.5 shows a 65% increase of PG/PGMAX at SWFAC = 0.5.

5. Conclusions

Crop models typically account for water stress by penalizing carbon assimilation when water supply falls under a certain limit, and the implementation of this penalization is typically linear. This popular approach is very convenient and simple, but it does not lead toward a deeper understanding of water stress nor to a comprehensive simulation of the same.

We demonstrated the infeasibility of a linear relationship between photosynthesis and transpiration using simulations at leaf and crop scales. The two leaf-scale models (a one-dimensional conductance model and 2DLEAF) showed that transpiration

response to changes in stomatal aperture/conductance is stronger than that of photosynthesis. At the crop-level, simulations of biomass, PESW, and pod yield in rainfed experiments improved significantly when we replaced the linear relationship linking photosynthesis and the satisfaction of potential transpiration requirements originally implemented in PNUTGRO with a nonlinear equation.

According to our results, WUE is a nonlinear function that increases under conditions of water stress. This finding is supported by experimental evidence (in peanut and other crops) found in the literature, and by theory integrating the quasi-steady-state stomatal closure due to low soil water availability, short-timescale midday adaptive behavior, and peanut-specific drought-avoidance mechanisms.

There are still many possible advances in crop modeling to be made by linking leaf and canopy gas exchange processes, as shown by Tanaka (2002). Our study did not incorporate a leaf-level gas exchange model into a crop model as done, for example, by Larocque (2002); the PNUTGRO model is not hierarchical as defined by Wu and David (2002), but the structure of its descendant CSM (Jones et al., 2003) is far more modular and hierarchical, and the lessons learned from this exercise with PNUTGRO could easily be implemented in that model.

Acknowledgements

We gratefully acknowledge the assistance of Marta Vinocur, who provided the Río Cuarto data, and of an anonymous reviewer for his/her valuable comments and suggestions. We are also grateful to the Florida Chapter of Phi Kappa Phi for partial funding of this project through R.A. Ferreyra's UF 2001-2002 Graduate Student Scholarship. R.A. Ferreyra also wishes to thank CEPROCOR (Córdoba, Argentina) for funding the 1996–1998 M.Sc. program that provided the original opportunity for this study, and the University of Florida's College of Agricultural and Life Sciences for its assistance through an Alumni Graduate Fellowship.

References

Abbate, P.E., Dardanelli, J.L., Cantarero, M.G., Maturano, M., Melchiori, R.J.M., Suero, E.E., 2002. Climatic environment and water availability effects on wheat water use efficiency. Crop Sci., in press.

Acock, B., Trent, A., 1991. The Soybean Crop Simulator, GLYCIM: Documentation for the Modular Version 91. Department of Plant, Soil and Entomological Sciences, University of Idaho, Moscow, Idaho, 242 pp.

American Institute of Physics Handbook, 3rd ed., vol. 1, 1972. McGraw-Hill, New York, 250 pp.

Antipov, N.I., 1971. Correlation between cuticular and stomatal transpiration in woody and bushy plants. Soviet Plant Physiol. 18 (6), 1026–1030.

Antipov, N.I., 1978. Intensity of the cuticular transpiration of grasses in different ecological conditions. In: Problems of Drought Tolerance of Plants. Moscow, Nauka, 227 pp. (in Russian).

Bhagsari, A.S., Brown, R.H., 1976a. Photosynthesis in peanut (*Arachis*) genotypes. Peanut Sci. 3, 1–5.

Bhagsari, A.S., Brown, R.H., 1976b. Relationship of net photosynthesis to carbon dioxide concentration and leaf characteristics in selected peanut (*Arachis*) genotypes. Peanut Sci. 3, 10–14.

Boote, K.J, Loomis, R.S., 1991. The prediction of canopy assimilation. In: Boote, K.J., Loomis, R.S. (Eds.), Modeling Crop Photosynthesis—From Biochemistry to Canopy. CSSA Special Publication Number 19. ASA, CSSA, SSSA, Madison, WI, pp. 109–140.

Boote, K.J., Jones, J.W., Hoogenboom, G., Wilkerson, G.G., Jagtap, S.S., 1989. PNUTGRO v. 1.02. Peanut Crop Growth Simulation Model. User's Guide. Florida Agricultural Experiment Station Journal Series No. 8420. University of Florida, Gainesville, FL.

Boote, K.J., Jones, J.W., Pickering, N.B., 1996. Potential uses and limitations of crop models. Agron. J. 88 (5), 704–716.

Boote, K.J., Jones, J.W., Hoogenboom, G., Wilkerson, G.G., 1997. Evaluation of the CROPGRO-Soybean model over a wide range of experiments. In: Kropff, M.J., et al. (Eds.), Applications of Systems Approaches at the Field Level, vol. 2. Kluwer, Dordrecht, pp. 113–133.

Boote, K.J., Jones, J.W., Hoogenboom and G., Pickering, N.B., 1998. The CROPGRO model for grain legumes. In: Tsuji, G.Y., Hoogenboom, G., Thornton P.K. (Eds.), Understanding Options for Agricultural Production. Kluwer Academic Publishers, Dordrecht, pp. 99–128.

Boughton, W.C., 1989. Review of the USDA SCS curve number method. Aust. J. Soil Res. 27 (3), 511–523.

Calmon, M.A., Jones, J.W., Shinde, D., Specht, J.E., 1999. Estimating parameters for soil water balance models using adaptive simulated annealing. Appl. Eng. Agric. 15 (6), 706–713.

Collino, D., Biderbost, E., Racca, R.W., 1994. Identificación y caracterización de variables fisiológicas para la selección de materiales tolerantes a la sequía en maní (*Arachis hypogaea* L.). Avances en Investigación en Maní, pp. 25–31.

Collino, D.J., Dardanelli, J.L., Sereno, R., Racca, R.W., 2000. Physiological responses of argentine peanut varieties to water stress. Water uptake and water use efficiency. Field Crops Res. 68, 133–142.

Craufurd, P.Q., Wheeler, T.R., Ellis, R.H., Sommerfield, R.J., Williams, J.H., 1999. Effect of temperature and water deficit on

water-use efficiency, carbon isotope discrimination, and specific leaf area in peanut. Crop Sci. 39, 136–142.

de Wit, C.T., 1982. Simulation of living systems. In: Penning de Vries, F.W.T., van Laar, H.H. (Eds.), Simulation of Plant Growth and Crop Production. Pudoc, Wageningen, The Netherlands, pp. 3–8.

Farquhar, G.D., von Caemmerer, S., Berry, J.A., 1980. A biochemical model of photosynthetic CO_2 assimilation in leaves of C3 species. Planta 149, 78–90.

Ferreyra, R.A., 1998. Development of a methodology for the quantitative identification and description of zones suitable for the peanut (*Arachis hypogaea* L.) crop using a crop simulation model. M.S. Thesis, Escuela para Graduados, Fac. de Cs. Agropecuarias, Universidad Nacional de Cordoba, Argentina (in Spanish).

Ferreyra, R.A., Pachepsky, L.B., Collino, D., Acock, B., 2000. Modeling peanut leaf gas exchange for the calibration of crop models for different cultivars. Ecol. Model. 131, 285–298.

Hall, A.J., Rebella, C.M., Ghersa, C.M., Culot, J. Ph., 1992. Field-crop systems of the Pampas. In: Pearson, C.J. (Ed.), Ecosystems of the World: Field Crop Ecosystems. Elsevier, Amsterdam, pp. 413–449.

Hammer, G.L., Kropff, M.J., Sinclair, T.R., Porter, J.R., 2002. Future contributions of crop modelling—from heuristics and supporting decision making to understanding genetic regulation and aiding crop improvement. Eur. J. Agron. 18 (1/2), 15–31.

Hanks, J., Ritchie, J.T. (Eds.), 1991. Modeling Plant and Soil Systems. ASA-CSSA-SSSA, Madison, WI.

Harley, P.C., Tenhunen, J.D., 1991. Modeling the photosynthetic response of C3 leaves to environmental factors. In: Boote, K.J., Loomis, R.S. (Eds.), Modeling Crop Photosynthesis—From Biochemistry to Canopy. CSSA Special Publication Number 19. CSSA, Madison, WI, pp. 17–39.

Jones, J.W., Hoogenboom, G., Porter, C.H., Boote, K.J., Batchelor, W.D., Hunt, L.A., Wilkens, P.W., Singh, U., Gijsman, A.J., Ritchie, J.T., 2003. The DSSAT cropping system model. Eur. J. Agron. 18 (3/4), 235–265.

Jørgensen, S.E., 2002. Explanation of ecological rules and observation by application of ecosystem theory and ecological models. Ecol. Model. 158, 241–248.

Keating, B.A., Carberry, P.S., Hammer, G.L., Probert, M.E., Robertson, M.J., Holzworth, D., Huth, N.I., Hargreaves, J.N.G., Meinke, H., Hochman, Z., McLean, G., Verburg, K., Snow, V., Dimes, J.P., Silburn, M., Wang, E., Brown, S., Bristow, K.L., Asseng, S., Chapman, S., McCown, R.L., Freebairn, D.M., Smith, C.J., 2003. An overview of APSIM, a model designed for farming systems simulation. Eur. J. Agron. 18 (3/4), 267–288.

Larcher, W., 1995. Physiological Plant Ecology, 3rd ed. Springer, NY, 506 pp.

Larocque, G.R., 2002. Coupling a detailed photosynthetic model with foliage distribution and light attenuation functions to compute daily gross photosynthesis in sugar maple (*Acer saccharum* Marsh.) stands. Ecol. Model. 148, 213–232.

Ma, Y., Sawhney, V.K., Steves, T.A., 1992. Staining of paraffin embedded plant material in safranin and fast-green without removal of the paraffin. Can. J. Bot. 71, 996–999.

Marques, J.C., Jørgensen, S.E., 2002. Three selected ecological observations interpreted in terms of a thermodynamic hypothesis. Contribution to a general theoretical framework. Ecol. Model. 158, 213–221.

Mavromatis, T., Boote, K.J., Jones, J.W., Irmak, A., Shinde, D., Hoogenboom, G., 2001. Developing genetic coefficients for crop simulation models with data from crop performance trials. Crop Sci. 41 (1), 40–51.

Nobel, P.S., 1983. Biophysical Plant Physiology and Ecology. W.H. Freeman & Co., NY, 608 pp.

Pachepsky, L.B., Acock, B., 1996. A model 2DLEAF of leaf gas exchange: development, validation, and ecological application. Ecol. Model. 93, 1–18.

Pachepsky, L.B., Haskett, J.D., Acock, B., 1995. A two-dimensional model of leaf gas exchange with special reference to leaf anatomy. J. Biogeogr. 22, 209–214.

Pachepsky, L.B., Acock, B., Hoffman-Benning, S., Willmitzer, L., Fisahn, J., 1997. Estimation of the anatomical, stomatal and biochemical components of differences in photosynthesis and transpiration of wild-type and transgenic (expressing yeast-derived invertase targeted to the vacuole) tobacco leaves. Plant Cell Environ. 20, 1070–1078.

Pachepsky, L.B., Ferreyra, R.A., Collino, D., Acock, B., 1999. Transpiration rates and leaf boundary layer parameters for peanut analyzed with the two-dimensional model 2DLEAF. Biotronics 28, 1–12.

Pallas Jr., J.E., 1980. An apparent anomaly in peanut leaf conductance. Plant Physiol. 65 (5), 848–851.

Parkhurst, D.F., 1994. Diffusion of CO_2 and other gases inside leaves. Tansley review no. 65. New Phytol. 120, 449–479.

Pedelini, R., 1991. La produccion manisera en la Argentina. Panorama Manisero 15, 15–27.

Penning de Vries, F.W.T., Brunstin, A.H., van Laar, H.H., 1974. Products, requirements and efficiency of biosynthesis —quantitative approach. J. Theor. Biol. 45 (2), 339–377.

Penning de Vries, F.W.T., Jansen, D.M., ten Berge, H.F.M., Bakema, A., 1989. Simulation of Ecophysiological Processes of Growth in Several Annual Crops. Simulation Monographs 29. Pudoc-DLO, Wageningen, The Netherlands, 308 pp.

Poluektov, R.A., Topaj, A.G., 2001. Crop modeling: nostalgia about present and reminiscence about future. Agron. J. 93, 653–659.

Ravelo, A.C., Dardanelli, J.L., 1992. Calibración y validación de un modelo fisiológico para maní (*Arachis hypogaea*). Rev. Facultad de Agronomía 13 (1), 25–32.

Ritchie, J.T., 1981. Water dynamics in the soil-plant-atmosphere system. Plant Soil 55, 81–96.

Sakai, W.S., 1973. Simple method for differential staining of paraffin embedded plant material using toluidine blue O. Stain Technol. 48, 247–249.

Sau, F., Boote, K.J., Ruiz-Nogueira, B., 1999. Evaluation and improvement of CROPGRO-soybean model for a cool environment in Galicia, northwest Spain. Field Crops Res. 61 (3), 273–291.

Seiler, R.A., Vinocur, M.G., 1995. Evaluación de un modelo de rendimiento de maní como herramienta para la planificación y el manejo del cultivo. Agriscientia, XII (No especial), pp. 53–59.

Sinclair, T.R., Tanner, C.B., Bennett, J.M., 1984. Water-use efficiency in crop production. BioScience 34, 36–40.

Smartt, J., Stalker, H.T., 1982. Speciation and cytogenetics in *Arachis*. In Pattee, H.E., Young, C.T. (Eds.), Peanut Science and Technology. American Peanut Researches and Education Society, Yoakum, TX, pp. 21–49.

Soil Conservation Service, 1972. National Engineering Handbook, Hydrology Section 4, Chapters 4–10. USDA.

Tanaka, K., 2002. Multi-layer model of CO_2 exchange in a plant community coupled with the water budget of leaf surfaces. Ecol. Model. 147, 85–104.

Tang, Sh., Li, Y., Wang, Y., 2001. Simultaneous equations, error-in-variable models, and model integration in systems ecology. Ecol. Model. 142, 285–294.

Tanner, C.B., Sinclair, T.R., 1983. Efficient water use in crop production: research or re-search? In: Taylor, H.M., et al. (Eds.), Limitations to Efficient Water Use in Crop Production. American Society of Agron, Madison, WI, pp. 1–28.

Van den Berg, M., Driessen, P.M., Rabbinge, R., 2002. Water uptake in crop growth models for land use systems analysis: II. Comparison of three simple approaches. Ecol. Model. 148, 233–250.

Van Wijk, M.T., Bouten, W., Verstraten, J.M., 2002. Comparison of different modelling strategies for simulating gas exchange of a Douglas-fir forest. Ecol. Model. 158, 63–81.

Wright, G.C., Nageswara Rao, R.C., Farquhar, G.D., 1994. Water-use efficiency and carbon isotope discrimination in peanut under water deficit conditions. Crop Sci. 34, 92–97.

Wu, J., David, J.L., 2002. A spatially explicit hierarchical approach to modeling complex ecological systems: theory and applications. Ecol. Model. 153, 7–26.

Young, J.H., Cox, F.R., Martin, C.K., 1979. A peanut growth and development model. Peanut Sci. 6, 27–36.